Food Chemistry 395 (2022) 133564

Contents lists available at ScienceDirect

Food Chemistry

journal homepage: www.elsevier.com/locate/foodchem

Encapsulation of *Lactobacillus acidophilus* in solid lipid microparticles via cryomilling

Mehran Kazemi, Fakhri Shahidi *, Mohammad Javad Varidi *, Sahar Roshanak

Department of Food Science and Technology, Faculty of Agriculture, Ferdowsi University of Mashhad, Mashhad, Iran

ARTICLE INFO

Keywords:
Ball mill
Microencapsulation
Fat powder
Superfine cryogenic grinding
Probiotics

Chemical compounds studied in this article:
Stearic acid (PubChem CID: 5281)
Oleic acid (PubChem CID: 445639)

ABSTRACT

We herein delved into the microencapsulation of *Lactobacillus acidophilus* (LA) into solid lipid microparticles (SLMs) via the cryomilling technique. For this aim, a frozen lipid mixture containing LA was pulverized at different times (7, 14, 21, 28, and 35 min) using a cryogenic mixer mill to produce probiotic-loaded SLMs. The impacts of different cryomilling durations on the SLMs properties (morphology, particle size, water activity, polymorphism, crystallinity, and thermal behavior) and the viability of LA were evaluated. Microencapsulation improved the viability of LA in simulated gastrointestinal fluids, heat stress, and different concentrations of salt and sucrose. SLMs also were suitable to be incorporated into foods. However, once the cryomilling time was prolonged, the viability of encapsulated LA declined, and particle size grew. The cryomilling technique showed great potential as an alternative approach for encapsulation due to the lack of solvent, short processing time, and simplicity.

1. Introduction

The survival of probiotic bacteria is adversely influenced by various harsh conditions. Therefore, effective techniques such as microencapsulation of probiotics have been adopted to prolong cell viability (Chen et al., 2017). In this regard, solid lipid microparticles (SLMs) have been proposed as the promising wall materials to protect probiotics against detrimental conditions (de Matos-Jr et al., 2019; Okuro et al., 2013; de Pedroso et al., 2012; Silva et al., 2018), and also have great potential as an alternative to conventional colloidal carriers (Miao et al., 2016; Okuro et al., 2013).

One of the advantages of the lipid-based microcapsules over the polysaccharide-based carriers is that they can protect probiotics against harsh gastric conditions more sufficiently because lipases do not exist in gastric fluid. Instead, the intestinal lipases digest lipid-based shells and release the core cells in the adjacency of the site of their action (Favaro-Trindade et al., 2011). The techniques that have recently been employed for encapsulation of probiotics within SLMs are spray chilling (Okuro et al., 2013; de Pedroso et al., 2012; Silva et al., 2018) and complex coacervation (de Matos-Jr et al., 2019; Tasch Holkem & Favaro-Trindade, 2020).

Water activity plays a substantial role in the viability of encapsulated probiotics during storage, and high water activities aggravate mortality of bacteria by increasing their metabolic activity (Okuro et al., 2013; Šipailienė & Petraitytė, 2018). It was reported that SLMs acquired by the spray chilling technique possessed a high water activity (a_w) because this method is performed through cold atomization, which is a physical process whereby water is not removed (Silva et al., 2018). The complex coacervation technique is not merely intricate to scale-up but also needs an aqueous solution; consequently, it requires an extra drying process to prolong the shelf life of samples (Favaro-Trindade et al., 2011). Herein, therefore, we cast light on a simple yet innovative top-down approach for the encapsulation of probiotics to surmount the above-mentioned obstacles associated with the conventional techniques.

Ball milling is a straightforward and environment-friendly method that works based upon impact force and attrition resulting from the collision of balls with milling materials and the inner wall of the jars (Gao et al., 2020). Ball mills can be operated in varying levels of energy (low energy or high energy milling), different mediums (wet or dry milling), and various temperatures (high temperature, room temperature, or cryomilling).

Cryomilling is a type of mechanical grinding method that performs at temperatures lower than −150 °C using liquid nitrogen or liquid argon (Katiyar et al., 2020). This technique is tailored to elastic and thermosensitive compounds, and does not solely prevent the loss of heat-sensitive ingredients but provides better retention of particle size

* Corresponding authors at: Department of Food Science and Technology, Faculty of Agriculture, Ferdowsi University of Mashhad, Iran.
E-mail addresses: fshahidi@um.ac.ir (F. Shahidi), mjvaridi@um.ac.ir (M. Javad Varidi).

https://doi.org/10.1016/j.foodchem.2022.133564
Received 17 February 2022; Received in revised form 18 June 2022; Accepted 21 June 2022
Available online 24 June 2022

distribution, color, volatile components, and biological activities (Gao et al., 2020). There is a dearth of evidence concerning the microencapsulation of probiotic bacteria by the cryomilling technique, and to the best of our knowledge, this is the first investigation conducted for this aim.

Incorporating a high percentage of saturated fatty acids in SLMs is indispensable for the fabrication of the firm and consistent SLMs to ensure high physical resistance and ease of handling and storage of them (Oriani et al., 2018). Among various saturated fatty acids, increased amounts of circulating dietary stearic acid are interestingly connected with reduced blood pressure, enhanced heart function, and diminished cancer risk. Consequently, as opposed to other saturated fatty acids and in contrast with the general belief that saturated fatty acids are unhealthy, stearic acid has beneficial impacts on human health (Senyilmaz-Tiebe et al., 2018). It might be due to the fact that stearic acid can be metabolized quickly to oleic acid via ubiquitous Δ9-desaturase (Gunstone, 2008). Moreover, stearic acid is generally considered one of the cheapest and the most accessible saturated fatty acids (Scrimgeour & Harwood, 2007). Therefore, in the present study, a high portion of SLMs was made of stearic acid.

The objectives of the present paper were to a) entrap the *lactobacillus acidophilus* into SLMs via pulverizing the frozen fat matrix containing probiotic bacteria using the cryomill, b) characterize the SLMs obtained at different processing times, and c) determine the viability of bacteria during storage, under stress conditions, and in simulated gastric and intestinal fluid.

2. Materials and methods

2.1. Materials

Lactobacillus acidophilus (IBRC-M 10815) was procured from the Iranian Biological Resource Center, Tehran, Iran. Oleic acid and stearic acid were purchased from Merck (Darmstadt, Germany), pancreatin from the porcine pancreas, trypsin from the bovine pancreas, and pepsin from porcine gastric mucosa were obtained from Sigma-Aldrich (St. Louis, MO, USA).

2.2. Preparation of probiotic bacteria

The *L. acidophilus* culture was activated in 10 mL of MRS broth at 37 °C for 18 h. A small portion of activated *Lactobacillus acidophilus* culture was inoculated in 90 mL of MRS broth and incubated for 18 h at 37 °C (Silva et al., 2018). Afterward, *L. acidophilus* was centrifuged at 4000 rpm for 10 min, and the resulting pellet was washed twice with phosphate buffer saline (PBS) solution and resuspended at a concentration of approximately 10^9 CFU/mL prior to encapsulation.

2.3. Determination of surface hydrophobicity of bacteria

The surface hydrophobicity (SH) of *L. acidophilus* was determined through bacterial adhesion to hydrocarbons as described by Ahimou et al. (2001), with minor modifications. The obtained pellet was washed twice with phosphate buffer saline, and it was suspended in the same buffer to attain a concentration of approximately 10^8 CFU/mL. Thereafter, the optical density (D0) was adjusted to 0.25 at 600 nm to standardize the number of bacteria. Then, 3 mL of the bacterial suspension was accompanied by 0.15 mL of toluene for bacteria to adhere to this aromatic hydrocarbon. Next, vortexing was implemented for 2 min before phase separation (one hour at room temperature). Subsequently, the aqueous phase was carefully removed by a sterile pipet, and its absorbance (D1) was recorded at 600 nm. SH% was calculated by the Eq. (1):

$$SH\% = (1 - D1/D0) \times 100 \quad (1)$$

Where D0 and D1 were the absorbances before and after adding the toluene, respectively.

2.4. Encapsulation of bacteria in SLMs by cryomilling technique

L. acidophilus was prepared according to section 2.2 and was added to the stearic acid/oleic acid (SA/OA) mixture with an 80:20 ratio, which was melted at 10 °C above its melting point (48.8 °C). According to Morselli Ribeiro et al. (2012), based on the melting point and stability of SLMs, different ratios of SA/OA, including 70:30, 80:20, 90:10, and 100:0, can be chosen for the binary lipid mixture. The SA/OA with an 80:20 ratio was selected to produce the SLMs in this study because the higher percentage of oleic acid (30%) in SLMs may lead to faster oxidation during storage (Oriani et al., 2018). On the other hand, the higher percentages of stearic acid (90% and 100%) in SLMs possibly can accelerate the formation of β crystals throughout storage (Ramel et al., 2016). Additionally, Morselli Ribeiro et al. (2012) and Yuan et al. (2007) reported that the formulation of lipid particles containing 20% oleic acid exhibited a high encapsulation efficiency.

The suspension of bacteria and molten lipid was mixed using a homogenizer (Fine Tech, Shin Saeng, Korea) at 4000 rpm for 60 s at a temperature above the melting point of the SA/OA. Subsequently, the beaker that contained the mixture was immersed directly in liquid nitrogen (-196 °C) kept in a Styrofoam box without any controlled nucleation, long enough (approximately 15 min) to ensure that thermal equilibrium was completely achieved. Later, the frozen lipid was precrushed manually to be prepared for the cryomilling process ahead.

The cryogenic mixer mill (NARYA-BM 25, Amin Asia Fanavar Pars, Karaj, Iran) with two stainless steel cups, each having a volume of 25 cc with an inner diameter of 12 mm along with two stainless steel balls (each ball had a diameter of 10 mm and weighed 9 g) was utilized to produce probiotic-loaded SLMs via powdering the frozen lipid matrix containing probiotics. The injection of liquid nitrogen was simultaneous with the cryomilling process. To find the proper range of cryomilling time, first, cryomilling was performed for 15, 30, 45, and 60 min at 40 rpm. A perceptible powder agglomeration that prevented free-flowing of powder was observed when samples were cryomilled for 45 and 60 min (data not shown). Thus, to avoid this undesirable phenomenon, the cryomilling was finally operated at a speed of 40 rpm for 7 min (T1), 14 min (T2), 21 min (T3), 28 min (T4), and 35 min (T5). Then, the effect of different cryomilling times on the properties of SLMs and the viability of encapsulated bacteria in various conditions were analyzed.

2.5. Characterization of SLMs

2.5.1. Determination of morphology

Scanning electron microscopy (SEM) (Stereoscan 360, Leica Cambridge, UK) at a 20 kV acceleration voltage with the amplitude of 200×, 500×, and 1000 × was utilized to assess the morphology of SLMs. Carbon sticky tabs were coated with a gold layer attached to aluminum stubs. Afterward, microparticles were sprinkled over the stubs, and surplus SLMs were blown away.

2.5.2. Particle size analysis

The particle size distribution and volume-weighted mean diameter (D (4,3)) of SLMs were determined via OMEC LS-909 laser diffraction particle size analyzer (OMEC Instrument Co., Jinding Harbour Avenue, Zhuhai, Guangdong, China). The SLMs produced by the cryomilling technique were fully dispersed in water because, according to Cain et al. (2002), the free-flowing fat powder yielded by means of cryomill possessed a high dispersibility in cold water. The polydispersity index (span) of particles was measured by Eq. (2). Particle size measurements were carried out in triplicate at room temperature.

$$Span = (d_{90} - d_{10})/d_{50} \quad (2)$$

2.5.3. Evaluation of polymorphism and crystallinity

The Philips X-ray diffractometer (PW3710, Netherland) was utilized at room temperature to determine the polymorphism of SLMs after 90 days of storage at 7 °C by running the powder samples in the 2θ that ranged from 5 to 35° under X-ray generated through Cu Kα source (λ = 1.54056 Å), a voltage of 40 kV, a current of 30 mA, and an angular velocity of 0.04°/s. The crystallinity of various samples were evaluated via OriginPro version 9.6.5 (OriginLab Corporation, Northampton, MA, USA). First, the diffractogram of each sample was smoothed by 15 points, then the area of crystalline peaks (AC) and total area of peaks (TA) were measured by the software. Finally, the percentage of crystallinity of each sample was calculated by Eq. (3).

$$Crystallinity(\%) = (AC/TA) \times 100 \quad (3)$$

2.5.4. Assessment of water activity (a_w)

Water activity (a_w) of various powder samples obtained via the cryomilling process was determined by the water activity meter of LabMaster-aw (Novasina AG, Lachen, Switzerland).

2.5.5. Differential scanning calorimetry (DSC) analysis

In order to determine the thermal properties of samples by means of the Mettler Toledo DSC 1 (Mettler Toledo, Schwerzenbach, Switzerland), 10 mg of each sample were hermetically sealed within an aluminum capsule and heated at a rate of 10 °C/min from −50 to 100 °C in an inert N_2 atmosphere (45 mL/min) (Okuro et al., 2013).

2.6. Viability of bacteria after encapsulation and during storage

After encapsulation, the number of viable *L. acidophilus* was assessed by the pour plate culturing on MRS agar plates (DeMan Rogosa and Sharp) (Okuro et al., 2013). Briefly, one gram of SLMs was added to 9 mL of sodium citrate and heated to 59 ± 1 °C. Next, the released bacteria were serially diluted in tubes containing warm 2% sodium citrate, then pure plated, and incubated in microaerophilic conditions at 37 °C ± 1 °C for 72 h. SLMs samples were stored at 7 °C in sealed glass jars deprived of exposure to light without controlling the presence of oxygen and humidity for 8 weeks. The viability of encapsulated *L. acidophilus* was evaluated at days 0, 14, 28, 42, and 56 as described above. The viability of encapsulated bacteria at day 0 was determined immediately after the encapsulation process, and the encapsulation yield (EY) (%) was calculated according to Eq. (4). Survival rate of bacteria during storage was measured by Eq. (5).

$$Encapsulationyield(\%) = (N/N_o) \times 100 \quad (4)$$

Where N is the viable encapsulated cell count (log CFU/g) released from SLMs, and N_o is the initial free viable cell count (log CFU/g) before being added to the molten fat.

$$Survivalrate(\%) = (V/V_o) \times 100 \quad (5)$$

Where V_o is the viable cell count after encapsulation at day 0 (log CFU/g), and V is the viable cell count (log CFU/g) during storage.

2.7. Survival of microencapsulated cells under the stress conditions

The effect of pH, NaCl, sucrose, and temperature on the survival of encapsulated probiotics was evaluated based upon the method proposed by Silva et al. (2018) with minor modifications. Briefly, 0.5 g of SLMs was suspended into 4.5 mL of 2% sodium citrate solutions that were adjusted to pH of 2 and 4.5 by hydrochloric acid (HCl). Afterward, the resistance of encapsulated and unencapsulated bacteria to pH was assessed after 3 h. For evaluating the effect of salt and sucrose on the survival of probiotics, 25% and 45% (w/v) of sucrose, and 3%, 6%, and 9% (w/v) of NaCl separately were dissolved in 4.5 mL of 2% sodium citrate solutions, and the viability of encapsulated and free cells was determined after 60 min. The effect of temperature was assessed by counting free and encapsulated bacteria after adding them to a tube containing 2% sodium citrate solution heated to 50 °C in a water bath for 60 min. The viability of bacteria after exposure to these stress conditions was determined according to section 2.2.

2.8. In vitro assessment of cells in gastric and intestinal fluid

In vitro evaluation of tolerance of free and encapsulated microorganisms in simulated gastric fluid (SGF) and simulated intestinal fluid (SIF) was conducted based upon the method proposed by Gbassi et al. (2009). For preparing the SGF, 9 g/L of sodium chloride and 3 g/L of pepsin from porcine stomach mucosa were added to distilled water, and then the pH was adjusted to 1.8 using HCl. Next, the SGF was agitated continuously at 50 rpm, and viability of the encapsulated bacteria and free cells was determined after 0, 60, and 120 min at 37 °C. The SIF was prepared by mixing 9 g/L of sodium chloride, 10 g/L of pancreatin, 10 g/L of bovine pancreas trypsin, and 3 g/L of bile salts with distilled water. Afterward, the pH was adjusted to 6.5 with sodium hydroxide, and the viable cells were counted after 0, 90, 180 min at 37 °C.

2.9. Statistical analysis

Analysis of variance (ANOVA) of the results obtained by measuring in triplicate was operated via SPSS software (Version 26.0, IBM SPSS Inc, USA). The significant differences were assessed by Duncan's test with a 95% confidence interval. The correlation between the particle size and the viability of encapsulated cells was calculated based on the Pearson correlation coefficient via SPSS software.

3. Results and discussion

3.1. Surface hydrophobicity (SH) of bacteria

SH of probiotic strains is classified into three groups, including low hydrophobicity (0–35%), medium hydrophobicity (36–70%), and high hydrophobicity (71–100%) (Samot et al., 2011). The SH of *L. acidophilus* measured in this study was 35.73% ± 1.28, which is categorized between the low and medium hydrophobicity groups. Colloca et al. (2000) determined the SH of *L. acidophilus* by toluene and reported that the SH of bacteria isolated from tongue, teeth, and saliva was 77%, 64%, and 73%, respectively. The SH of *L. acidophilus* studied in the current study differed because each bacterial strain has a specific SH on account of its various intrinsic factors (cell-wall composition: proteins, glycoproteins, teichoic, and lipoteichoic acids) and extrinsic factors (differences in pH and temperature) (Tasch Holkem & Favaro-Trindade, 2020).

Since probiotics were entrapped in lipid particles, determination of the SH was essential to assure a more effective encapsulation or retention efficiency of cells within the SLMs (Silva et al., 2018). Furthermore, the SH and adhesion of probiotics can be beneficial for the host by improving the interactions between bacteria and the intestinal epithelial cells, thereby increasing probiotic colonization within the intestine (de Matos-Jr et al., 2019). Although SH of probiotics is considered beneficial, this should not set a limit on opting for encapsulation of strains owing to the fact that each strain confers various benefits on intestinal microbiota population, absorption of nutrients, water and electrolytes, body antioxidative capacity, and immune response (Tasch Holkem & Favaro-Trindade, 2020; Tuo et al., 2013).

3.2. Characteristics of SLMs

3.2.1. Morphology

Fig. 1A illustrates that the SLMs produced via cryomilling technique had irregular shapes; uneven and knobby surfaces with several pores and fissures; moreover, the agglomeration of SLMs is detectable. Different cryomilling times, ranging from 7 min to 35 min, did not lead

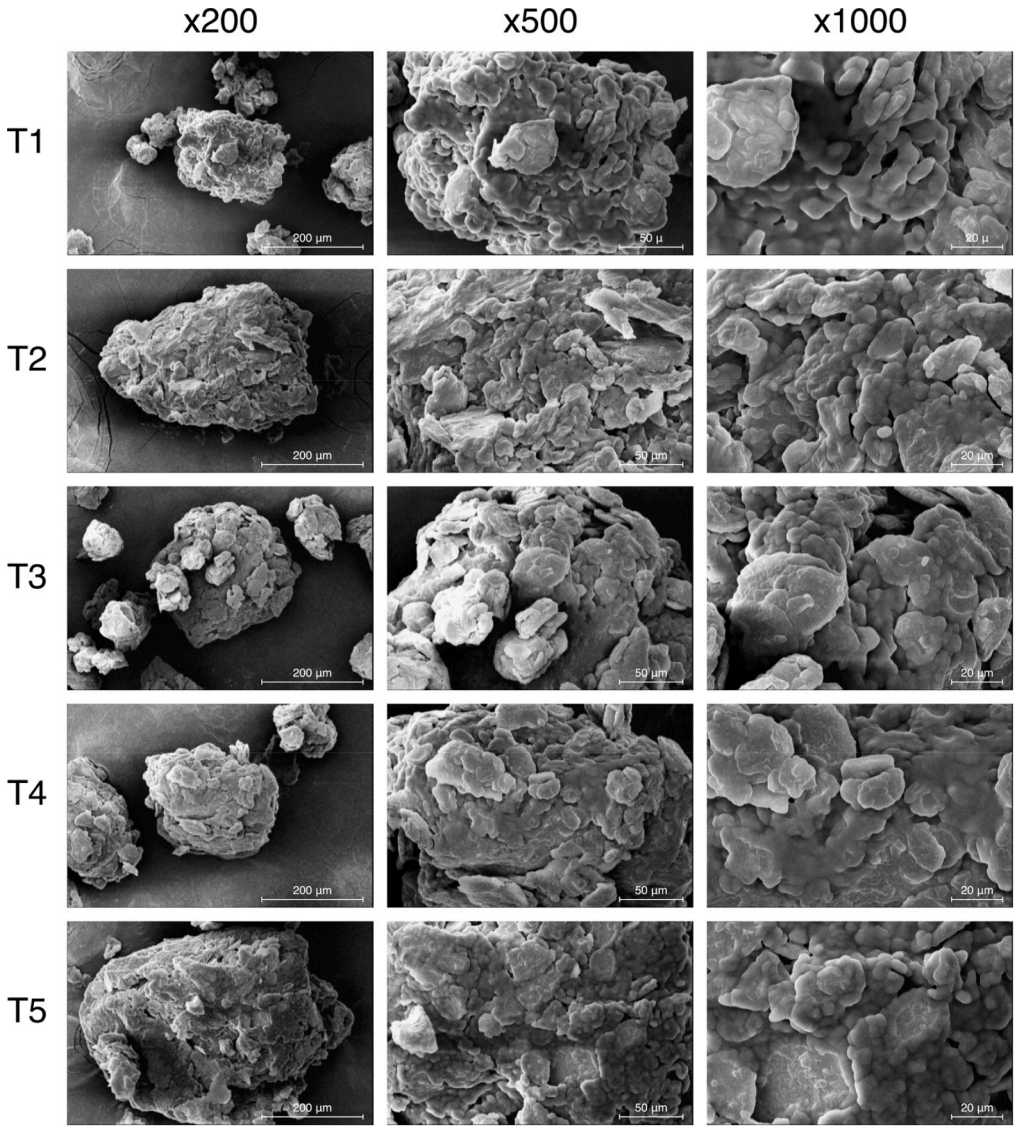

Fig. 1. (A) Scanning electron microscopy images (magnification x200, x500, and x1000) of solid lipid microparticles containing L. acidophilus. (B) Particle size distribution of probiotic-loaded SLMs yielded using cryomilling.

to any tangible differences in the morphology of samples. Besides, the analysis of SEM images using ImageJ software by thresholding technique (Gonzales-Barron & Butler, 2006) showed that the porosity of T1-T5 samples did not vary significantly.

The morphology of okara (a byproduct of the soybean industry) treated by the wet media planetary ball mill (Yang et al., 2021) bore a close resemblance to the morphology of SLMs yielded in this study. Nonetheless, it was reported that SLMs obtained through spray chilling had spherical shapes with relatively smooth and intact surfaces without pores or cracks (Okuro et al., 2013; de Pedroso et al., 2012). The dissimilarity between SLMs morphology revealed in different studies was attributed to the various strategies adopted for the microencapsulation of bacteria. Indeed, spray chilling is a technique whereby spherical SLMs form after atomization of molten fat through a narrow orifice toward a cold chamber, while cryomilling is a method in which the impact forces and attrition effect, resulting from movements of balls, randomly break the brittle chunks of lipid solidified by liquid nitrogen into smaller asymmetrical particles during the process.

3.2.2. Particle size

Volume-weighted mean diameter (D (4,3)), percentile values (d_{10}, d_{50}, d_{90}), and polydispersity index (span) of SLMs obtained using cryomilling are shown in Table 1. D (4,3) of SLMs ranged from 10.359 ± 0.440 μm to 85.101 ± 6.131 μm, corresponding to T1 and T5, respectively. Considering that the particles smaller than approximately 100 μm do not have a deteriorative impact on food texture (de Pedroso et al., 2012), the SLMs obtained by cryomilling are suitable for food applications. Because the finest particles are more preferred for food applications, cryomilling for 7 min (T1) was the most appropriate condition for encapsulation of the probiotics.

The particle size of SLMs increased by extending the cryomilling time. In fact, cryomilling produces momentary minuscule particles possessing high surface energies and large specific surface areas; subsequently, these tiny particles give rise to an agglomeration due to the high inter-particulate cohesive forces between them (Che et al., 2007; Loh et al., 2015). At the end of milling duration, the fracturing of the large agglomerates and the re-agglomeration of small particles achieve a dynamic equilibrium state that determines an apparent final size distribution (Che et al., 2007). Once the milling time is prolonged, the agglomeration of particles might occur more often than the fracturing of them (Loh et al., 2015), thereby increasing the particle size. Hence, the processing time is considered one of the milling conditions which governs the particle size of cryomilled substances. This explication is concurrent with the finding of Otte and Carvajal (2011) who reported that whereas cryomilling durations up to 5 min led to a reduction in particle size, processing time longer than 5 min did not cause any fracturing of particles but instead an increase in particle size.

Nevertheless, De Bondt et al. (2020) found that when the wheat bran was cryomilled for 30 min, the particle size was diminished to a median (d_{50}) of 6 μm. Their results were in contrast to our finding on account of the different nature of materials opted for cryomilling. In other words, particle size does not merely rely on the milling time but also on intrinsic factors such as the composition of cryomilled material. For instance, Pas et al. (2020) observed growth in particle size of cryomilled bovine serum albumin due to the occurrence of agglomeration; however, the particle size of gelatin 50PS was declined after cryomilling at the same conditions.

The spans of T3, T4, and T5 were significantly less than T1 and T2. Besides, there were no statistically considerable differences between spans of the T3, T4, and T5. The d_{10} of SLMs cryomilled for 7 and 14 min were 0.511 ± 0.024 μm and 0.602 ± 0.016 μm, respectively, and when cryomilling time is increased, these tiny particles tend to agglomerate as a result of their high surface energies and large specific surface areas. Accordingly, once cryomilling was performed for 21 min, those minuscule particles produced during the first 14 min of cryomilling started congregating, and formed bigger particles in the T3 sample. At this time, the d_{10} of T3 (22.493 ± 1.708 μm) became dramatically higher than the d_{10} of T2 (0.602 ± 0.016 μm). Thus, according to Eq. (2), the difference between d_{10} and d_{90} of the T3 particles became less than T2, which means that the T3 had a significantly smaller span and a narrower particle size distribution compared to the T2. It is also evident from Fig. 1B that the three short conspicuous peaks of each T1 and T2, which represent the distribution of particles smaller than approximately 10 μm, cannot be observed in the particle size distribution of T3, T4, and T5. Moreover, despite the T5 that had a bimodal size distribution, T4 and T3 had an asymmetrical monomodal size distribution.

3.2.3. Water activity

Evaluation of the water activity (a_w) is pivotal because high a_w of microcapsules can exacerbate the loss of microbial viability throughout subsequent storage on account of a rise in molecular mobility and metabolism (Okuro et al., 2013; Šipailienė & Petraitytė, 2018). For instance, Kurtmann et al. (2009) elucidated that the viability of freeze-dried *Lactobacillus acidophilus* in a sucrose or lactose matrix at a_w of 0.11 was higher compared to a_w of 0.23 and 0.43 at the same conditions (20 °C during 10 weeks of storage), regardless of matrix compositions.

The a_w of SLMs obtained via cryomilling ranged between 0.856 ± 0.007 and 0.694 ± 0.008, corresponding to T1 and T5, respectively. The T5 had the lowest a_w in light of the longer cryomilling time that led to more sublimation. Silva et al. (2018) stated that the a_w of SLMs yielded using the spray chiller was between 0.911 and 0.984, which was higher than a_w of SLMs produced by cryomilling. Because, water is neither evaporated nor sublimated during the spray chilling (Silva et al., 2018), but it can be partially sublimated throughout the cryomilling process. However, those authors reported that a_w of freeze-dried SLMs covered by gelatin and gum Arabic ranged from 0.245 to 0.326. Even though freeze-drying could bring about less a_w in comparison to cryomilling, freeze-drying is much more time-consuming.

3.2.4. Polymorphism, crystallinity

Crystalline polymorphism is a phenomenon wherein different structures of lipid crystals can exist based upon their arrangement, and each form has various thermodynamic and physicochemical properties. Fats mainly have three polymorphic forms, including α (metastable), β' (intermediate stable), and β (stable), in which there is an irreversible transition from a less stable form towards a more stable form (McClements, 2012). As shown in Fig. 2A, the two intense peaks for short spacing (d) of 0.42 and 0.38 nm at angles of approximately $2\theta = 21°$ and

Table 1
Encapsulation yield, particle size analysis, and water activity of SLMs.

SLMs	EY (%)	D (4,3) (μm)	d_{10} (μm)	d_{50} (μm)	d_{90} (μm)	Span	a_w
T1	90.66 ± 0.12 ^{a}	10.359 ± 0.440 ^{a}	0.511 ± 0.024 ^{a}	10.784 ± 0.391 ^{a}	20.896 ± 0.938 ^{a}	1.890 ± 0.030 ^{a}	0.856 ± 0.007 ^{a}
T2	90.46 ± 0.13 ^{a}	20.314 ± 3.205^{b}	0.602 ± 0.016 ^{a}	20.180 ± 3.245^{b}	39.459 ± 5.572^{b}	1.929 ± 0.046 ^{a}	0.706 ± 0.007^{c}
T3	87.87 ± 0.16^{b}	64.091 ± 6.551^{c}	22.493 ± 1.708^{c}	60.015 ± 1.416^{c}	103.002 ± 4.175^{c}	1.341 ± 0.067^{b}	0.737 ± 0.006^{b}
T4	84.04 ± 0.40^{c}	71.851 ± 4.576^{c}	17.729 ± 0.380^{b}	73.361 ± 3.895 ^{d}	121.971 ± 10.484 ^{d}	1.419 ± 0.075^{b}	0.716 ± 0.005^{c}
T5	82.97 ± 0.09 ^{d}	85.101 ± 6.131 ^{d}	24.055 ± 1.182^{c}	94.034 ± 2.667 ^{e}	138.000 ± 5.657 ^{e}	1.304 ± 0.178^{b}	0.694 ± 0.008 ^{d}

Values with the same upper-case letter within a column are not statistically different ($p > 0.05$). T1, T2, T3, T4, and T5 are samples cryomilled for 7 min, 14 min, 21 min, 28 min, and 35 min, respectively. D (4,3) demonstrates volume-weighted diameter. d_{10}, d_{50}, and d_{90} correspond to 10%, 50%, and 90% of the cumulative volume (%) of the microparticles, respectively. Span denotes polydispersity index of SLMs. a_w stands for water activity of carriers.

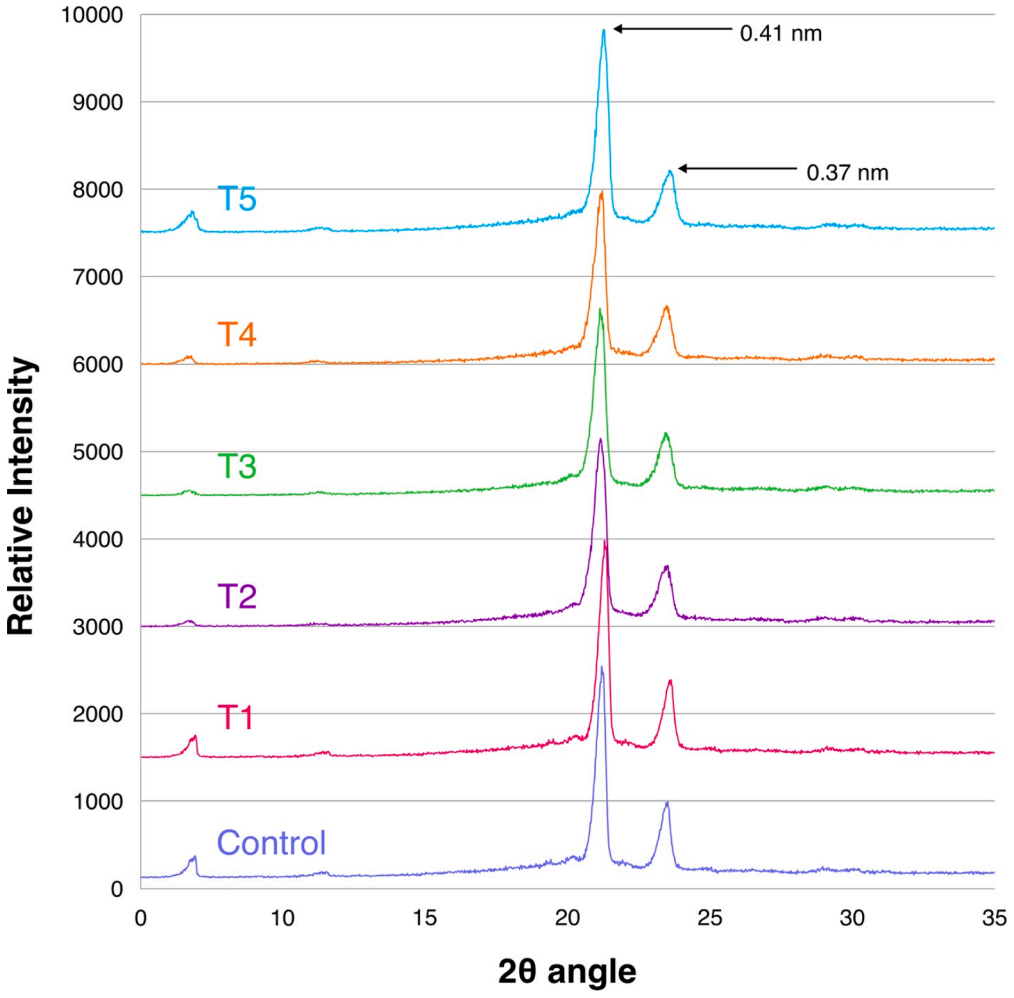

Fig. 2. (A) X-ray diffraction pattern of SLMs produced by cryomilling. (B) Differential scanning calorimetry (DSC) results for the control sample (bulk solid lipid contained probiotics before cryomilling) and SLMs loaded probiotics.

23° revealed that the main polymorphic form was β' in all samples after storing at 7 °C for 90 days (Basso et al., 2010). The β' crystals are smaller and softer compared to the β form; therefore, the SLMs produced via the cryomilling technique can be used in food matrices without deterioration of food texture (Paucar et al., 2016).

The small-angle region between 1 and 15°represents long spacing and depends on the length of TAG molecules (Acevedo, 2018). The TAGs can be arranged in triple chain-length (3L) or double chain-length (2L) structures, and the former has a higher long spacing (Metin & Hartel, 2020). In the current study, the long spacing value for samples was 1.4 nm, demonstrating the presence of 2L-structure crystals (Meng et al., 2011). The 2L structure was observed in this study because, despite 3L crystals, the 2L crystals are generally formed by fatty acids that have similar chain lengths (Sato, 2018).

Since the polymorphism plays a significant role in SLMs properties after 90 days of storage, the XRD analysis was not conducted immediately in this study. Hence, there could be two possibilities with regard to the formation of crystalline structures, including the process conditions and cold storage (Salvim et al., 2015). Despite a slow-cooling rate that causes the arrangement of more stable polymorphic forms, a fast-cooling rate prompts the formation of the least stable forms (Ramel et al., 2016). For instance, Campos et al. (2002) found that while the β' was obtained through a fast crystallization of lard fat, the predominant forms were β' + β when a slow crystallization occurred. In the current study, therefore, the α crystals were possibly the main polymorphic form during cryomilling due to the fast-cooling rate of the process and the presence of oleic acid in SLMs. Nonetheless, α crystals are not stable; consequently, there was a transition toward a more stable form (β') throughout storage. Moreover, due to the low percentage of oleic acid in SLMs, β crystals were not observed after 90 days of storage. Indeed, the *cis*-unsaturated fatty acid chains of oleic acid tend to be less compact owing to a double bond at C-9; hence, making the crystal lattice less ordered and inhibiting the formation of β crystals in SLMs (Ramel et al., 2016). Likewise, Oriani et al. (2016) reported that when a low percentage of oleic acid was incorporated in SLMs, it influenced palmitic acid crystal structures in a way that the predominant polymorphic form in SLMs was β'.

According to Fig. 2A, there was not any notable alteration in the polymorphic form, peak height, and peak width among diffractograms of different SLMs samples. The crystallinity of all the samples had a strong resemblance to each other, ranging from approximately 36% to 40%. Accordingly, the low speed of cryomilling used in the present study did not induce a considerable change in the crystallinity of SLMs.

3.2.5. Thermal behavior

Fig. 2B illustrates the thermal behavior of the samples. The melting point of SLMs was almost similar, ranging from 49.30 °C to 50.93 °C. The melting point of bulk solid lipid (the control sample) was 55.03 °C, while SLMs demonstrated lower melting points because, according to the relation between the particle size and melting point stated by Thomson (Eq. (6)), once the size reduction occurs in bulk materials, the melting temperature of the obtained particles diminished (Akhoond Zardini et al., 2018).

$$LnT/T_0 = 2\gamma V_s/r\Delta H \quad (6)$$

Where T and T_0 are the melting points of particle and bulk material, respectively, r is the particle radius, ΔH is molar melting enthalpy, γ is interfacial energy, and V_s is molar volume of the material (Akhoond Zardini et al., 2018).

The enthalpy of the control sample was similar to the enthalpy of stearic/oleic acid (80:20) reported by Morselli Ribeiro et al. (2012). When the cryomilling was performed for 7 min, the enthalpy declined from 140.69 J/g in bulk solid lipid to 115.34 J/g in the T1 sample owing to the sharp size reduction (Akhoond Zardini et al., 2018; Bunjes, 2011; Zhong & Zhang, 2019). Then, by increasing the cryomilling time, the melting enthalpy of T2-T5 increased in comparison with the T1, probably because when surface energy increased as a result of extended cryomilling time, as explained in the section 3.2.2, the size of SLMs was grown on account of the Van der Waals interaction and aggregation between particles (Sato, 2018; Che et al., 2007; Loh et al., 2015). Therefore, the enthalpy energy rose in T2-T5 samples compared to the T1 due to the particle size growth and increased surface energy (Eq. (6)) (Akhoond Zardini et al., 2018; Bunjes, 2011; Zhong & Zhang, 2019). The melting enthalpy of T2-T5 samples was relatively similar. It is worth noting that since the crystallinity and polymorphic form of samples did not differ among samples, they could not markedly influence the melting behavior of SLMs.

3.3. Viability of encapsulated cells after the process and throughout storage

The lowest and the highest EY% of encapsulated bacteria after cryomilling belonged to T5 and T1, corresponding to 82.97% and 90.66%, respectively (Table 1). The EY% was decreased significantly by prolonging the milling time on account of an increase in cell destruction exerted by the impact force of balls during the process. Based on the Pearson analysis, a significant negative correlation with the coefficient of −0.926 was observed between particle size and the viability of cells after encapsulation. Likewise, H. Wang et al. (2020) stated that once ball milling duration was prolonged, the viability of bacteria declined owing to the increase in cell-wall breakage ratio and gDNA leakage from microbial cells. In the current study, if cryomilling speed had been increased, cell mortality would have been aggravated. Hence, the moderate speed of cryomilling was performed for a short period to cushion the adverse effect of the encapsulation process on the probiotic viability.

The results of the viability evaluation of encapsulated bacteria during 56 days of storage at 7 °C are represented in Table 2. Humidity and the presence of oxygen were not controlled during storage due to the simulation of actual conditions associated with food applications. The average number of viable encapsulated cells among all treatments after the 56 days of storage period was 7.466 ± 0.451 log CFU/g, which is considered an acceptable number of viable probiotics to provide health benefits for consumers (Frakolaki et al., 2020). After 56 days of storage, the survival rates of cells loaded into T1, T2, and T3 were 91.65%, 91.77%, and 95.42%, respectively. Even though T4 and T5 had lower a_w compared to the T1, T2, and T3, surprisingly, encapsulated bacteria in these samples showed survival rates of 89.81% and 87.09%, respectively. The lower a_w was supposed to give rise to a better survival rate of encapsulated *L. acidophilus*, but a longer cryomilling time unexpectedly suppressed the beneficial impact of low a_w on the viability of encapsulated probiotics during storage. Indeed, increasing cryomilling time induces more mechanical stress to the cellular membrane, thus increasing

Table 2
The viability of encapsulated L. acidophilus during 56 days of storage at 7 °C.

	The viability during storage (log CFU/g)				
SLMs	**Day 0**	**Day 14**	**Day 28**	**Day 42**	**Day 56**
T1	8.159 ± 0.011^{Aa}	7.934 ± 0.015^{Ab}	7.859 ± 0.021^{Ab}	7.593 ± 0.104^{Bc}	7.478 ± 0.068^{Ad}
T2	8.141 ± 0.011^{Aa}	7.935 ± 0.024^{Ab}	7.853 ± 0.029^{Ac}	7.625 ± 0.040^{Bd}	7.471 ± 0.044^{Ae}
T3	7.575 ± 0.014^{Ba}	7.760 ± 0.034^{Bb}	7.599 ± 0.060^{Bc}	7.713 ± 0.012^{Ad}	7.228 ± 0.010^{Be}
T4	7.563 ± 0.036^{Ca}	7.440 ± 0.047^{Db}	7.261 ± 0.015^{Cc}	6.828 ± 0.050^{Cd}	6.792 ± 0.021^{Cd}
T5	7.467 ± 0.009^{Da}	7.678 ± 0.010^{Cb}	7.066 ± 0.024^{Dc}	6.530 ± 0.033^{Dd}	6.503 ± 0.048^{Dd}

Values with the same upper-case letter within a column and values with the same lower-case letter in a row are not statistically different ($p > 0.05$). T1, T2, T3, T4, and T5 are samples cryomilled for 7 min, 14 min, 21 min, 28 min, and 35 min, respectively.

the sensitivity of bacteria and diminishing their resistance against undesirable conditions (presence of oxygen and humidity) throughout storage. Likewise, Borges et al. (2016) elucidated that grinding negatively influenced the viability of probiotics during storage due to mechanical stress that was exerted on cells.

Zhang et al. (2020) utilized maltodextrin as a wall material for microencapsulation of probiotics (*L. Plantarum* P8 and *L. rhamnosus* GG) using freeze-drying followed by grinding. These authors reported that the viability of encapsulated cells declined by 0.3 log CFU/g after 6 weeks of storage at 4 °C. Nonetheless, the diminution in the viability of probiotics loaded into SLMs by cryomilling was higher after 6 weeks of storage, possibly due to the higher a_w of these SLMs. de Pedroso et al. (2012) found that when *L. acidophilus* was encapsulated via the spray chiller, viable cells were decreased by 3.81 log CFU/g after 60 days of storage at 7 °C. In another study with a similar encapsulation method, Okuro et al. (2013) enhanced the viability of encapsulated bacteria throughout the storage by reducing the a_w of SLMs thanks to adding prebiotics into the formulation, albeit the mortality of encapsulated bacteria reported by them was still higher during storage in comparison to the findings of the current study owing to the higher a_w of SLMs produced via spray chilling.

Silva et al. (2018) proposed that, during storage, the decline in the population of probiotics loaded into SLMs produced by spray chilling might not only arise from the higher a_w of SLMs but also depends on the microstructure of SLMs, in which probiotics mainly distribute on the surface of them, and consequently they come into contact with deteriorative factors more frequently than internal cells. In the present study, the presence of numerous pores and fissures on the surface of SLMs might allow various detrimental factors, including oxygen and humidity, to come into contact with encapsulated *L. acidophilus* during storage.

3.4. Resistance of free and encapsulated probiotics under stress conditions

The ability of encapsulated and free *L. acidophilus* to withstand sucrose, NaCl, and temperature are presented in Table 3. Loss of viability among encapsulated bacteria was significantly less than free cells in the presence of 25% and 45% sucrose after 1 h because SLMs impeded the osmotic pressure imposed by the sucrose solution. The reduction in both free and encapsulated bacteria in 45% sucrose solution was higher than 25% sucrose solution, owing to the higher osmotic stress. Likewise, Silva et al. (2018) reported that SLMs significantly shielded *L. acidophilus* LA3 and *Bifidobacterium animalis* subsp. lactis BLC1 from different concentrations of sucrose (25% and 45%).

Table 3
The loss of free and encapsulated L. acidophilus that was subjected to different pH for 180 min, sucrose solutions for 60 min, NaCl solutions for 60 min, and the heat treatment for 60 min.

	Loss of viability under different harsh conditions (log CFU/g)					
SLMs	**Sucrose (25%)**	**Sucrose (45%)**	**NaCl (3%)**	**NaCl (6%)**	**NaCl (9%)**	**Heat (50 °C)**
T1	0.023 ± 0.024 ^{a}	0.300 ± 0.025 ^{a}	0.012 ± 0.015 ^{ab}	0.446 ± 0.023^{b}	0.652 ± 0.024 ^{a}	0.053 ± 0.022 ^{a}
T2	0.062 ± 0.011 ^{ab}	0.341 ± 0.024 ^{a}	0.033 ± 0.017 ^{bc}	0.454 ± 0.017^{b}	0.691 ± 0.032 ^{a}	0.110 ± 0.024 ^{a}
T3	0.054 ± 0.043 ^{ab}	0.339 ± 0.031 ^{a}	0.005 ± 0.007 ^{a}	0.451 ± 0.042^{b}	0.845 ± 0.066^{b}	0.087 ± 0.026 ^{a}
T4	0.141 ± 0.022^{c}	0.344 ± 0.066 ^{a}	0.038 ± 0.006^{c}	0.364 ± 0.036 ^{a}	1.081 ± 0.018^{c}	0.105 ± 0.036 ^{a}
T5	0.098 ± 0.039 ^{bc}	0.314 ± 0.050 ^{a}	0.022 ± 0.015 ^{abc}	0.733 ± 0.014^{c}	1.193 ± 0.042 ^{d}	0.058 ± 0.044 ^{a}
Control	0.361 ± 0.008 ^{d}	1.301 ± 0.032^{b}	0.138 ± 0.011 ^{d}	1.910 ± 0.047 ^{d}	2.267 ± 0.023 ^{e}	0.775 ± 0.094^{b}

Values with the same upper-case letter within a column are not statistically different ($p > 0.05$). T1, T2, T3, T4, and T5 are samples cryomilled for 7 min, 14 min, 21 min, 28 min, and 35 min, respectively.

The resistance of encapsulated probiotics to 3%, 6%, and 9% of NaCl was significantly higher than unencapsulated cells. In consonance with the current study, Silva et al. (2018) reported that SLMs shielded probiotics markedly at various concentrations of NaCl (3%, 6%, and 9%). In another study, de Matos-Jr et al. (2019) stated that after 120 min of exposing probiotics to the concentration of 5% NaCl, the decrease in the population of *L. paracasei* BGP1 encapsulated into SLMs covered by gelatin and gum Arabic and free *L. paracasei* BGP1 was 0.41 CFU/mL and 2.23 log CFU/mL, respectively. Despite the presence of an external layer on those SLMs, which is expected to protect the bacteria more sufficiently than uncoated SLMs, their results were somewhat similar to the findings of the current study because the stability of the coacervate was compromised by ionic force, and the membrane formed by the gelatin-gum Arabic complex was then degraded (de Matos-Jr et al., 2019).

The viability of encapsulated bacteria at 50 °C after 60 min was considerably higher than free cells, and there were no significant differences between the survival of different encapsulated probiotics. By heating the probiotic-loaded SLMs composed of stearic acid and oleic acid at 50 °C, the microparticles were melted. Subsequently, the bacteria released into the medium were more susceptible to the detrimental impact of temperature (Silva et al., 2018), but others that were not released throughout heating had better survival than free cells due to the protective function of the lipid matrices against heat treatment. In this regard, the protective mechanism of SLMs against heat treatment stems from the fact that SLMs partially absorb the heat energy due to the solid-to-liquid phase transition of SLMs. This phenomenon might bring about a decrease in the internal temperature, hence alleviating the heat shock to the probiotics (Liu et al., 2015). In agreement with the present research, Silva et al. (2018) demonstrated that *L. acidophilus* encapsulated into SLMs had a survival rate of approximately 90% at 50 °C after 60 min, while the survival rate of free cells was 80%. Moreover, H. Liu et al. (2015) reported that once the ratio of a low melting point fat as a core material to wall material was increased from 0.25 to 1.00, the survival rate of *Lactobacillus zeae* LB1 was improved from 16% to 63% against the thermal in spray-dryer.

Survival of encapsulated and free cells in pH of 2 and 4.5 are illustrated in Fig. 3A. After 3 h exposing samples to a pH of 2, the loss of all encapsulated and free bacteria was significant. At this pH, the survival rate of the free probiotics was 72%, while encapsulated cells had a survival rate of approximately 90% on the grounds that lipid matrices shielded probiotics from direct exposure to the stressor of H^+ (de Pedroso et al., 2012). Therefore, these results elucidated that the encapsulation of *L. acidophilus* into SLMs by the cryomilling technique would significantly shelter cells from too low pH in highly acidic food matrices. However, at a pH of 4.5, the population of probiotics encapsulated in T4 and T5 decreased considerably, owing to the impact of longer cryomilling time as described in section 3.3.

3.5. Survival of encapsulated probiotics under simulated gastrointestinal conditions

Encapsulation is deemed a practical approach for the protection of probiotics against the presence of enzymes, low pH, and bile salts in the gastrointestinal tract (Cook et al., 2012; Silva et al., 2018). The resistance of the free and encapsulated *L. acidophilus* subjected to simulated gastric fluid (SGF) and simulated intestinal fluid (SIF) is shown in Fig. 3B. It can be inferred that the encapsulation via the cryomilling technique preserved the probiotics significantly compared to the free cells against simulated gastrointestinal fluids (SGI) during 300 min (SGF + SIF). The reduction in the population of encapsulated cells in the SGI was 3.61 log CFU/g (a survival rate of 54%), whereas 6.47 log CFU/g of the free *L. acidophilus* died (a survival rate of 23%) after exposure to the

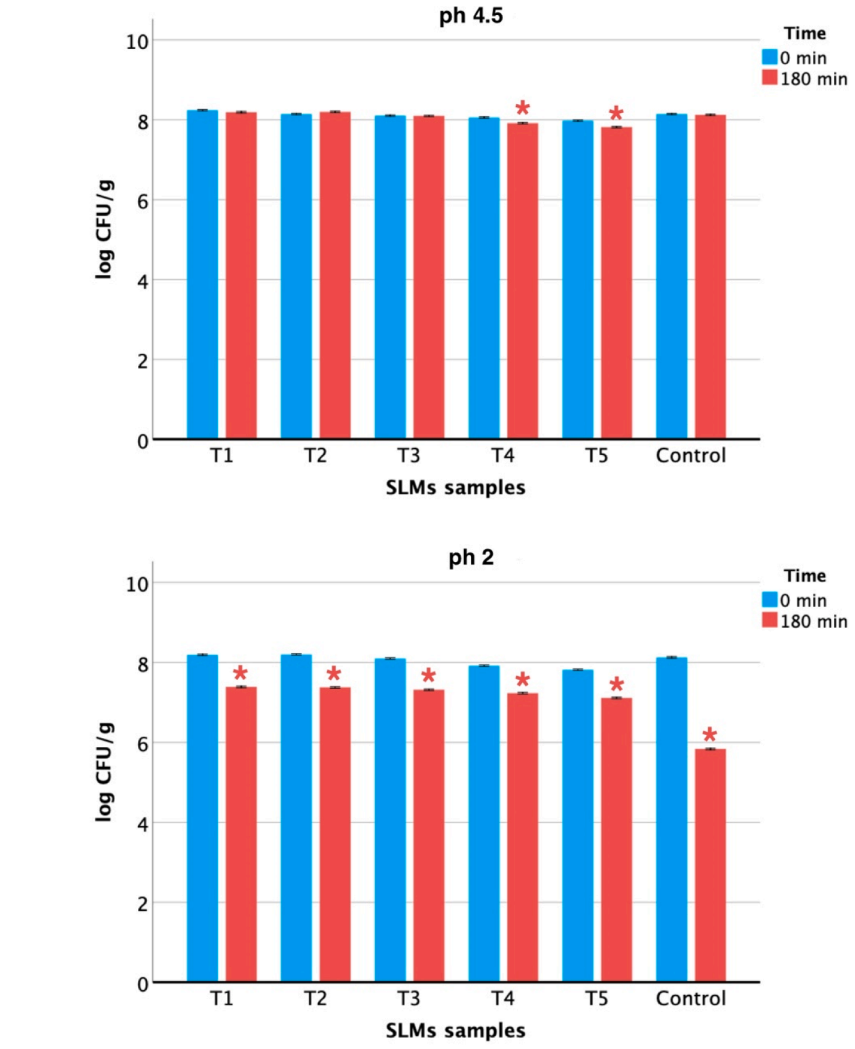

(A)

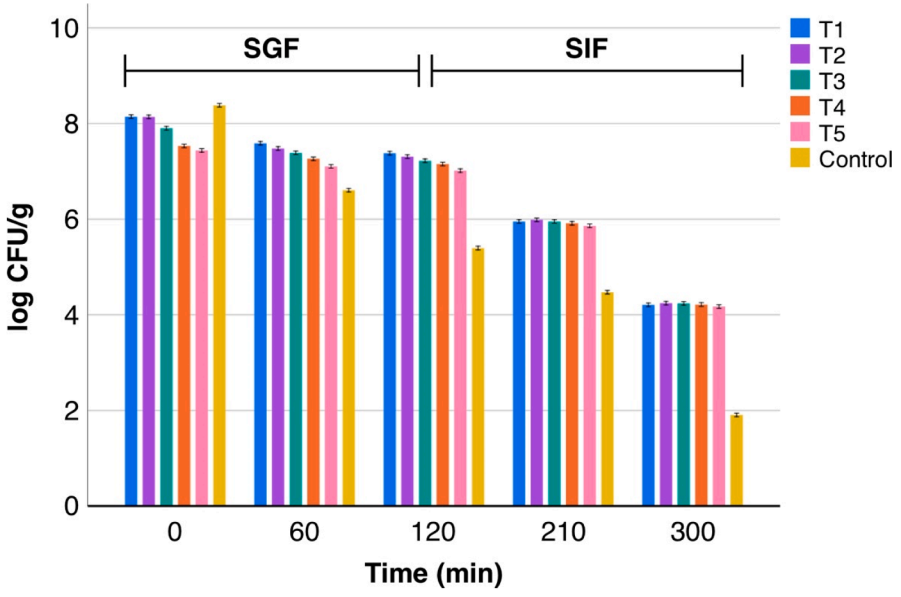

(B)

Fig. 3. (A) Effect of pH of 4.5 and 2 on survival of encapsulated and free L. acidophilus. (B) Survival of free and encapsulated L. acidophilus under simulated gastric fluid (SGF) and simulated intestine fluid (SIF).

SGI. Likewise, Okuro et al. (2013) demonstrated that while free cells were not detectable after the SGI assay, the SLMs could preserve approximately 60% of *L. acidophilus* after 300 min.

Notwithstanding that a decrement in the population of free probiotics exposed to the SGF was approximately 3 log CFU/g (a survival rate of 71%) after 120 min, the number of encapsulated bacteria diminished by 0.615 log CFU/g (a survival rate of 92%) after 120 min of being subjected to the SGF. These results proved that encapsulation of bacteria into SLMs through cryomilling had a nontrivial protective impact on the survival of probiotics in SGF. Okuro et al. (2013) observed that *L. acidophilus* co-encapsulated with prebiotics in SLMs by spray chilling remained almost unchanged during the SGF assay. Silva et al. (2018) also reported that the viability of probiotics encapsulated into SLMs via spray chilling was almost intact under the SGF condition. The resistance of encapsulated probiotics against the SGF in this study was less than bacteria encapsulated using a spray chiller owing to the presence of fissures, pores, and cavities on the surface of SLMs produced by cryomilling, which facilitated the exposure of the encapsulated bacteria to SGF. In another study, Mokarram et al. (2009) found that after 60 min of evaluation of free and encapsulated bacteria in SGF, the number of viable *L. acidophilus* entrapped within uncoated calcium alginate beads, and the same beads coated by one or two layers of sodium alginate was depleted by 3.915 log CFU/g, 2.278 log CFU/g, and 1.325 log CFU/g, respectively. The reduction in the number of those probiotics loaded in uncoated and coated calcium alginate beads was higher in SGF compared to the decline of encapsulated cells in the present study, possibly due to the different protection mechanisms between lipid and alginate-based particles. In fact, it is assumed that the alginate particles can protect cells from low pH conditions through their buffering effect (Cook et al., 2012), while SLMs mainly limit the diffusion of SGF across the lipid particles (Chen et al., 2017).

The average population of encapsulated microorganisms was declined by approximately 3 log CFU/g (a survival rate of 58%) when they underwent the SIF for 180 min; whereas, this condition caused a diminution in the viable free cells by 3.48 log CFU/g (a survival rate of 35%). Thus, encapsulated probiotics had significantly better survival than the free cells in the SIF condition. The SIF had a higher deteriorative impact on the viability of bacteria-loaded SLMs in comparison to the SGF owing to the presence of pancreatin, trypsin, and bile salts in SIF, which gave rise to a breakdown of SLMs, then the encapsulated cells were more prone to come in contact with the SIF (Okuro et al., 2013). de Matos-Jr et al. (2019) claimed that the number of *Lactobacillus rhamnosus* 64 and *Lactobacillus paracasei* BGP1 loaded into SLMs covered by gelatin and gum Arabic diminished by 1.64 log CFU/g and 1.71 log CFU/g, respectively, after 180 min of being subjected to SIF. The cells encapsulated into SLMs covered by gelatin and gum Arabic showed higher resistance to SIF in comparison to the encapsulated probiotics in the current study, possibly due to the extra layers of gelatin and gum Arabic that protected probiotics against SIF more adequately.

4. Conclusion

The encapsulation of *L. acidophilus* into SLMs by means of cryomilling is a simple yet innovative method that can significantly protect bacteria against adverse environmental conditions, including simulated GIT, low pH, heat, and high concentration of salt and sugar. The survival rate of encapsulated probiotics after 56 days of storage was satisfactory to confer health benefits to consumers. Moreover, characteristics of SLMs, such as fine particle size and presence of β' crystals, showed that the probiotic-loaded SLMs produced using the cryomilling technique have the potential to enrich foods without marring their texture. The advantages of the cryomilling method for microencapsulation of probiotics were lack of solvent, short processing time, low temperature, and having a relatively simple procedure. Nevertheless, some of the drawbacks of the cryomilling were that once the processing time was prolonged, a) the agglomeration transpired owing to the inter-particulate cohesive forces between SLMs, and b) the viability of encapsulated bacteria declined on account of an increase in damages to the probiotics. Hence, because high speeds and increased durations of cryomilling can minimize the advantages of this technique, cryomilling should be operated at low energies and short periods for encapsulation of probiotics in future studies.

CRediT authorship contribution statement

Mehran Kazemi: Conceptualization, Methodology, Software, Formal analysis, Writing – original draft. **Fakhri Shahidi:** Supervision, Project administration, Funding acquisition. **Mohammad Javad Varidi:** Supervision, Project administration, Funding acquisition. **Sahar Roshanak:** Supervision, Resources, Writing – review & editing.

Declaration of Competing Interest

The authors declare that they have no known competing financial interests or personal relationships that could have appeared to influence the work reported in this paper.

Data availability

The authors do not have permission to share data.

Acknowledgements

The authors sincerely appreciate professor Dr. Reza Farhoosh and Vahid Behshad (M.Sc.), Department of Food Science and Technology, Ferdowsi University. The authors acknowledge the Ferdowsi University of Mashhad for the financial support (Grant number: 3/54712).

References

Acevedo, N. C. (2018). Characterization of the Nanostructure of Triacylglycerol Crystal Networks. In *Structure-Function Analysis of Edible Fats*. AOCS Press. https://doi.org/10.1016/B978-0-12-814041-3.00001-0.

Ahimou, F., Paquot, M., Jacques, P., Thonart, P., & Rouxhet, P. G. (2001). Influence of electrical properties on the evaluation of the surface hydrophobicity of Bacillus subtilis. *Journal of Microbiological Methods, 45*(2), 119–126. https://doi.org/10.1016/S0167-7012(01)00240-8

Akhoond Zardini, A., Mohebbi, M., Farhoosh, R., & Bolurian, S. (2018). Production and characterization of nanostructured lipid carriers and solid lipid nanoparticles containing lycopene for food fortification. *Journal of Food Science and Technology, 55*(1), 287–298. https://doi.org/10.1007/s13197-017-2937-5

Basso, R. C., Ribeiro, A. P. B., Masuchi, M. H., Gioielli, L. A., Gonçalves, L. A. G., dos Santos, A. O., … Grimaldi, R. (2010). Tripalmitin and monoacylglycerols as modifiers in the crystallisation of palm oil. *Food Chemistry, 122*(4), 1185–1192. https://doi.org/10.1016/j.foodchem.2010.03.113

Borges, S., Barbosa, J., Silva, J., Gomes, A. M., Pintado, M., Silva, C. L. M., … Teixeira, P. (2016). A feasibility study of Lactobacillus plantarum in fruit powders after processing and storage. *International Journal of Food Science and Technology, 51*(2), 381–388. https://doi.org/10.1111/ijfs.12975

Bunjes, H. (2011). Structural properties of solid lipid based colloidal drug delivery systems. *Current Opinion in Colloid and Interface Science, 16*(5), 405–411. https://doi.org/10.1016/j.cocis.2011.06.007

Cain, F. W., Dekker, W., & Moore, S. R. (2002). *Free flowing fat compositions, Patent No. US6340491B1*.

Campos, R., Narine, S., & Marangoni, A. (2002). Effect of cooling rate on the structure and mechanical properties of milk fat and lard. *Food Research International, 35*(10), 971–981. https://doi.org/10.1016/S0963-9969(02)00159-X

Che, L. M., Li, D., Wang, L. J., Chen, X. D., & Mao, Z. H. (2007). Micronization and Hydrophobic Modification of Cassava Starch. *International Journal of Food Properties, 10*(3), 527–536. https://doi.org/10.1080/10942910600932982

Chen, J., Wang, Q., Liu, C. M., & Gong, J. (2017). Issues deserve attention in encapsulating probiotics: Critical review of existing literature. *Critical Reviews in Food Science and Nutrition, 57*(6), 1228–1238. https://doi.org/10.1080/10408398.2014.977991

Colloca, M. E., Ahumada, M. C., López, M. E., & Nader-Macías, M. E. (2000). Surface properties of lactobacilli isolated from healthy subjects. *Oral Diseases, 6*(4), 227–233. https://doi.org/10.1111/j.1601-0825.2000.tb00118.x

Cook, M. T., Tzortzis, G., Charalampopoulos, D., & Khutoryanskiy, V. V. (2012). Microencapsulation of probiotics for gastrointestinal delivery. *Journal of Controlled Release, 162*(1), 56–67. https://doi.org/10.1016/j.jconrel.2012.06.003

De Bondt, Y., Liberloo, I., Roye, C., Windhab, E. J., Lamothe, L., King, R., & Courtin, C. M. (2020). The Effect of Wet Milling and Cryogenic Milling on the Structure and

Physicochemical Properties of Wheat Bran. *Foods, 9*(12), 1755. https://doi.org/10.3390/foods9121755

Favaro-Trindade, C. S., Heinemann, R. J. B., & Pedroso, D. L. (2011). Developments in probiotic encapsulation. In *CAB Reviews: Perspectives in Agriculture, Veterinary Science, Nutrition and Natural Resources* (Vol. 6, Issue 004). https://doi.org/10.1079/PAVSNNR20116004.

Frakolaki, G., Giannou, V., Kekos, D., & Tzia, C. (2020). A review of the microencapsulation techniques for the incorporation of probiotic bacteria in functional foods. In *Critical Reviews in Food Science and Nutrition* (Vol. 0, Issue 0, pp. 1–22). Taylor & Francis. https://doi.org/10.1080/10408398.2020.1761773.

Gao, W., Chen, F., Wang, X., & Meng, Q. (2020). Recent advances in processing food powders by using superfine grinding techniques: A review. *Comprehensive Reviews in Food Science and Food Safety, 19*(4), 2222–2255. https://doi.org/10.1111/1541-4337.12580

Gbassi, G. K., Vandamme, T., Ennahar, S., & Marchioni, E. (2009). Microencapsulation of Lactobacillus plantarum spp in an alginate matrix coated with whey proteins. *International Journal of Food Microbiology, 129*(1), 103–105. https://doi.org/10.1016/j.ijfoodmicro.2008.11.012

Gonzales-Barron, U., & Butler, F. (2006). A comparison of seven thresholding techniques with the k-means clustering algorithm for measurement of bread-crumb features by digital image analysis. *Journal of Food Engineering, 74*(2), 268–278. https://doi.org/10.1016/j.jfoodeng.2005.03.007

Gunstone, F. D. (2008). The chemical nature of lipids: Food industry briefing series. *Oils and fats in the food industry. www.wiley.com/wiley-blackwell*.

Katiyar, N. K., Biswas, K., & Tiwary, C. S. (2020). Cryomilling as environmentally friendly synthesis route to prepare nanomaterials. *International Materials Reviews*, 1–40. https://doi.org/10.1080/09506608.2020.1825175

Kurtmann, L., Carlsen, C. U., Skibsted, L. H., & Risbo, J. (2009). Water activity-temperature state diagrams of freeze-dried lactobacillus acidophilus (La-5): Influence of physical state on bacterial survival during storage. *Biotechnology Progress, 25*(1), 265–270. https://doi.org/10.1002/btpr.96

Liu, H., Gong, J., Chabot, D., Miller, S. S., Cui, S. W., Ma, J., … Wang, Q. (2015). Protection of heat-sensitive probiotic bacteria during spray-drying by sodium caseinate stabilized fat particles. *Food Hydrocolloids, 51*, 459–467. https://doi.org/10.1016/j.foodhyd.2015.05.015

Loh, Z. H., Samanta, A. K., & Sia Heng, P. W. (2015). Overview of milling techniques for improving the solubility of poorly water-soluble drugs. *Asian Journal of Pharmaceutical Sciences, 10*(4), 255–274. https://doi.org/10.1016/j.ajps.2014.12.006

Matos-Jr, F. E. de, Silva, M. P. da, Kasemodel, M. G. C., Santos, T. T., Burns, P., Reinheimer, J., Vinderola, G., & Favaro-Trindade, C. S. (2019). Evaluation of the viability and the preservation of the functionality of microencapsulated Lactobacillus paracasei BGP1 and Lactobacillus rhamnosus 64 in lipid particles coated by polymer electrostatic interaction. *Journal of Functional Foods, 54* (December 2018), 98–108. https://doi.org/10.1016/j.jff.2019.01.006.

McClements, D. J. (2012). Crystals and crystallization in oil-in-water emulsions: Implications for emulsion-based delivery systems. *Advances in Colloid and Interface Science, 174*, 1–30. https://doi.org/10.1016/j.cis.2012.03.002

Meng, Z., Liu, Y. F., Jin, Q. Z., Huang, J. H., Song, Z. H., Wang, F. Y., & Wang, X. G. (2011). Comparative analysis of lipid composition and thermal, polymorphic, and crystallization behaviors of granular crystals formed in beef tallow and palm oil. *Journal of Agricultural and Food Chemistry, 59*(4), 1432–1441. https://doi.org/10.1021/jf103875f

Metin, S., & Hartel, R. W. (2020). Fundamentals of Lipid Crystallization. *Bailey's Industrial Oil and Fat Products*. https://doi.org/10.1002/047167849X.bio021.pub2

Miao, Y., Jia, B., Chen, M., & Zhang, W. (2016). Preparation and characterization of solid lipid microparticles with liquid crystal structure. *Molecular Crystals and Liquid Crystals, 633*(1), 110–122. https://doi.org/10.1080/15421406.2016.1177899

Mokarram, R. R., Mortazavi, S. A., Najafi, M. B. H., & Shahidi, F. (2009). The influence of multi stage alginate coating on survivability of potential probiotic bacteria in simulated gastric and intestinal juice. *Food Research International, 42*(8), 1040–1045. https://doi.org/10.1016/j.foodres.2009.04.023

Morselli Ribeiro, M. D. M., Barrera Arellano, D., & Ferreira Grosso, C. R. (2012). The effect of adding oleic acid in the production of stearic acid lipid microparticles with a hydrophilic core by a spray-cooling process. *Food Research International, 47*(1), 38–44. https://doi.org/10.1016/j.foodres.2012.01.007

Okuro, P. K., Thomazini, M., Balieiro, J. C. C., Liberal, R. D. C. O., & Fávaro-Trindade, C. S. (2013). Co- encapsulation of Lactobacillus acidophilus with inulin or polydextrose in solid lipid microparticles provides protection and improves stability. *Food Research International, 53*(1), 96–103. https://doi.org/10.1016/j.foodres.2013.03.042

Oriani, V. B., Alvim, I. D., Consoli, L., Molina, G., Pastore, G. M., & Hubinger, M. D. (2016). Solid lipid microparticles produced by spray chilling technique to deliver ginger oleoresin: Structure and compound retention. *Food Research International, 80*, 41–49. https://doi.org/10.1016/j.foodres.2015.12.015

Oriani, V. B., Alvim, I. D., Paulino, B. N., Procópio, F. R., Pastore, G. M., & Hubinger, M. D. (2018). The influence of the storage temperature on the stability of lipid microparticles containing ginger oleoresin. *Food Research International, 109*, 472–480. https://doi.org/10.1016/j.foodres.2018.04.066

Otte, A., & Carvajal, M. T. (2011). Assessment of Milling-Induced Disorder of Two Pharmaceutical Compounds. *Journal of Pharmaceutical Sciences, 100*(5), 1793–1804. https://doi.org/10.1002/jps.22415

Pas, T., Bergonzi, A., Michiels, E., Rousseau, F., Schymkowitz, J., Koekoekx, R., … Van den Mooter, G. (2020). Preparation of Amorphous Solid Dispersions by Cryomilling: Chemical and Physical Concerns Related to Active Pharmaceutical Ingredients and Carriers. *Molecular Pharmaceutics, 17*(3), 1001–1013. https://doi.org/10.1021/acs.molpharmaceut.9b01265

Paucar, O. C., Tulini, F. L., Thomazini, M., Balieiro, J. C. C., Pallone, E. M. J. A., & Favaro-Trindade, C. S. (2016). Production by spray chilling and characterization of solid lipid microparticles loaded with vitamin D3. *Food and Bioproducts Processing, 100*, 344–350. https://doi.org/10.1016/j.fbp.2016.08.006

Pedroso, D. de L., Thomazini, M., Heinemann, R. J. B., & Favaro-Trindade, C. S. (2012). Protection of Bifidobacterium lactis and Lactobacillus acidophilus by microencapsulation using spray-chilling. *International Dairy Journal*, *26*(2), 127–132. https://doi.org/10.1016/j.idairyj.2012.04.008.

Ramel, P. R., Co, E. D., Acevedo, N. C., & Marangoni, A. G. (2016). Structure and functionality of nanostructured triacylglycerol crystal networks. *Progress in Lipid Research, 64*, 231–242. https://doi.org/10.1016/j.plipres.2016.09.004

Salvim, M. O., Thomazini, M., Pelaquim, F. P., Urbano, A., Moraes, I. C. F., & Favaro-Trindade, C. S. (2015). Production and structural characterization of solid lipid microparticles loaded with soybean protein hydrolysate. *Food Research International, 76*, 689–696. https://doi.org/10.1016/j.foodres.2015.08.003

Samot, J., Lebreton, J., & Badet, C. (2011). Adherence capacities of oral lactobacilli for potential probiotic purposes. *Anaerobe, 17*(2), 69–72. https://doi.org/10.1016/j.anaerobe.2011.04.001

Sato, K. (2018). Crystallization of Lipids: Fundamentals and Applications in Food, Cosmetics and Pharmaceuticals. In *Crystallization of Lipids: Fundamentals and Applications in Food, Cosmetics and Pharmaceuticals*. https://doi.org/10.1002/9781118593882.

Scrimgeour, C. M., & Harwood, J. L. (2007). Fatty Acid And Lipid Structure. In *The Lipid Handbook with CD-ROM, Third Edition*.

Senyilmaz-Tiebe, D., Pfaff, D. H., Virtue, S., Schwarz, K. V., Fleming, T., Altamura, S., … Teleman, A. A. (2018). Dietary stearic acid regulates mitochondria in vivo in humans. *Nature Communications, 9*(1), 3129. https://doi.org/10.1038/s41467-018-05614-6

Silva, M. P., Tulini, F. L., Matos-Jr, F. E., Oliveira, M. G., Thomazini, M., & Fávaro-Trindade, C. S. (2018). Application of spray chilling and electrostatic interaction to produce lipid microparticles loaded with probiotics as an alternative to improve resistance under stress conditions. *Food Hydrocolloids, 83*, 109–117. https://doi.org/10.1016/j.foodhyd.2018.05.001

Šipailienė, A., & Petraitytė, S. (2018). Encapsulation of Probiotics: Proper Selection of the Probiotic Strain and the Influence of Encapsulation Technology and Materials on the Viability of Encapsulated Microorganisms. In *Probiotics and Antimicrobial Proteins* (Vol. 10, Issue 1). https://doi.org/10.1007/s12602-017-9347-x.

Tasch Holkem, A., & Favaro-Trindade, C. S. (2020). Potential of solid lipid microparticles covered by the protein-polysaccharide complex for protection of probiotics and proanthocyanidin-rich cinnamon extract. *Food Research International, 136*(June), 109520. https://doi.org/10.1016/j.foodres.2020.109520

Tuo, Y., Yu, H., Ai, L., Wu, Z., Guo, B., & Chen, W. (2013). Aggregation and adhesion properties of 22 Lactobacillus strains. *Journal of Dairy Science, 96*(7), 4252–4257. https://doi.org/10.3168/jds.2013-6547

Wang, H., Tao, M., Zhang, H., Cheng, S., Zhang, L., & Liu, Z. (2020). The mechanism on decreasing the microbiological contamination of superfine green tea powder by ball milling. *LWT, 134*(July), 109966. https://doi.org/10.1016/j.lwt.2020.109966

Yang, T., Yan, H. L., & Tang, C. H. (2021). Wet media planetary ball milling remarkably improves functional and cholesterol-binding properties of okara. *Food Hydrocolloids*, *111*(October 2020), 106386. https://doi.org/10.1016/j.foodhyd.2020.106386.

Yuan, H., Wang, L. L., Du, Y. Z., You, J., Hu, F. Q., & Zeng, S. (2007). Preparation and characteristics of nanostructured lipid carriers for control-releasing progesterone by melt-emulsification. *Colloids and Surfaces B: Biointerfaces, 60*(2), 174–179. https://doi.org/10.1016/j.colsurfb.2007.06.011

Zhang, C., Quek, S. Y., Fu, N., Su, Y., Kilmartin, P. A., & Chen, X. D. (2020). Storage stability and in vitro digestion of microencapsulated powder containing fermented noni juice and probiotics. *Food Bioscience*, *37*(October 2019), 100740. https://doi.org/10.1016/j.fbio.2020.100740.

Zhong, Q., & Zhang, L. (2019). Nanoparticles fabricated from bulk solid lipids: Preparation, properties, and potential food applications. *Advances in Colloid and Interface Science, 273*, 102033. https://doi.org/10.1016/j.cis.2019.102033